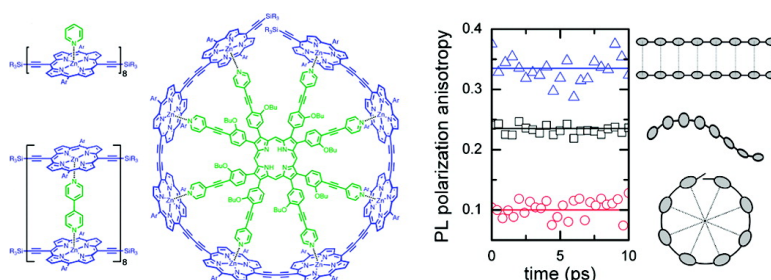


Dynamics of Excited-State Conformational Relaxation and Electronic Delocalization in Conjugated Porphyrin Oligomers

Ming-Hua Chang, Markus Hoffmann, Harry L. Anderson, and Laura M. Herz

J. Am. Chem. Soc., **2008**, 130 (31), 10171-10178 • DOI: 10.1021/ja711222c • Publication Date (Web): 10 July 2008

Downloaded from <http://pubs.acs.org> on February 8, 2009



More About This Article

Additional resources and features associated with this article are available within the HTML version:

- Supporting Information
- Links to the 2 articles that cite this article, as of the time of this article download
- Access to high resolution figures
- Links to articles and content related to this article
- Copyright permission to reproduce figures and/or text from this article

[View the Full Text HTML](#)

Dynamics of Excited-State Conformational Relaxation and Electronic Delocalization in Conjugated Porphyrin Oligomers

Ming-Hua Chang,[†] Markus Hoffmann,[‡] Harry L. Anderson,[‡] and Laura M. Herz^{*†}

Clarendon Laboratory, Department of Physics, University of Oxford, Parks Road, Oxford OX1 3PU, United Kingdom, and Chemistry Research Laboratory, Department of Chemistry, University of Oxford, Mansfield Road, Oxford OX1 3TA, United Kingdom

Received December 19, 2007; E-mail: l.herz@physics.ox.ac.uk

Abstract: We have investigated the influence of nuclear geometric relaxation on the extent of the excited-state electronic delocalization in conjugated zinc porphyrin oligomers using ultrafast transient photoluminescence spectroscopy. By use of metal-coordinating templates that force the oligomers into specific geometries in solution we are able to distinguish clearly between relaxation effects arising from the two vibrational modes that preferentially couple to the electronic transitions in such materials, i.e., carbon–carbon bond stretches and inter-ring torsions. We find that light absorption generates an excited state that is initially strongly delocalized along the oligomer but contracts rapidly following vibrational relaxation of the nuclei along C–C stretch coordinates on the subpicosecond time scale. We are able to monitor such excitonic self-trapping effects by observing the extent to which the concomitant ultrafast rotation of the transition dipole moment is found to correlate with the degree of bending induced in the molecular backbone. We further demonstrate that interporphyrin torsional relaxation leads to a subsequent increase in the excited-state electronic delocalization on a longer time scale (~ 100 ps). Such dynamic planarization of the molecular backbone is evident from the time-dependent increase in the overall emission intensity and red-shift in the peak emission energy that can be observed for wormlike flexible porphyrin octamers but not for torsionally rigidified cyclic or double-strand octamer complexes. These results therefore indicate that, following excitation, the initially highly delocalized excited-state wave function first contracts and then expands again along the conjugated backbone in accordance with the time periods for the vibrational modes coupled to the electronic transition.

Introduction

Conjugated molecular materials are highly attractive as active ingredients in electroluminescent devices,¹ solar cells,^{2,3} and transistors^{4,5} owing to their potential for cheap device fabrication directly from solution. Organic semiconductors fundamentally differ from their inorganic counterparts by having a significantly stronger electron–phonon coupling. Photoexcitation of a conjugated polymer or oligomer is therefore in general followed by strong geometric relaxation of the underlying nuclear framework, which in turn affects the delocalization of the excited-state wave function along the molecular backbone.^{6,7} However, the extent of such excitonic delocalization, and in particular its evolution over time, is currently the subject of much debate. An accurate analysis of these effects is complicated by the fact that geometric relaxation in conjugated

molecules occurs along a range of different configuration coordinates. For most conjugated polymers and oligomers significant changes in carbon–carbon bond-length alternations occur following a π – π^* transition.^{6,7} The geometric relaxation along the C–C stretch coordinates is expected to evolve on the time scale of the associated vibration period ($T \sim 25$ fs for a typical phonon energy of 1300 – 1600 cm^{-1}) and lead to rapid contraction of the excited-state wave function within the changed lattice potential, referred to as exciton “self-trapping”.^{7,8} However, it is becoming increasingly clear that electronic transitions in these materials also couple strongly to the slower torsional motion between extended conjugated units comprising the oligomer as, for example, phenyl, thiophene, or porphyrin rings.⁹ In general, steric constraints tend to force these molecules to adopt a twisted structure in the ground state with nonzero torsional angles between the ring components, whereas excitation leads to a strengthening of the inter-ring bonds and may cause a subsequent planarization of the molecular backbone.^{7,9}

[†] Department of Physics.

[‡] Department of Chemistry.

- (1) Friend, R. H.; Gymer, R. W.; Holmes, A. B.; Burroughes, J. H.; Marks, R. N.; Taliani, C.; Bradley, D. D. C.; Bredas, J. L.; Logdlund, M.; Salaneck, W. R. *Nature* **1999**, *397*, 121–128.
- (2) Snaith, H. J.; Arias, A. C.; Morteani, A. C.; Silva, C.; Friend, R. H. *Nano Lett.* **2002**, *2*, 1353–1357.
- (3) Morteani, A. C.; Sreearunothai, P.; Herz, L. M.; Friend, R. H.; Silva, C. *Phys. Rev. Lett.* **2004**, *92*, 247402.
- (4) Sirringhaus, H.; Kawase, T.; Friend, R. H.; Shimoda, T.; Inbasekaran, M.; Wu, W.; Woo, E. P. *Science* **2000**, *290*, 2123–2126.
- (5) Lloyd-Hughes, J.; Richards, T.; Sirringhaus, H.; Castro-Camus, E.; Herz, L. M.; Johnston, M. B. *Appl. Phys. Lett.* **2006**, *89*, 112101.

- (6) Cornil, J.; Beljonne, D.; Heller, C. M.; Campbell, I. H.; Laurich, B. K.; Smith, D. L.; Bradley, D. D. C.; Müllen, K.; Brédas, J. L. *Chem. Phys. Lett.* **1997**, *278*, 139–145.
- (7) Tretiak, S.; Saxena, A.; Martin, R. L.; Bishop, A. R. *Phys. Rev. Lett.* **2002**, *89*, 097402.
- (8) Ruseckas, A.; Wood, P.; Samuel, I. D. W.; Webster, G. R.; Mitchell, W. J.; Burn, P. L.; Sundstrom, V. *Phys. Rev. B* **2005**, *72*, 115214.
- (9) Karabunarliev, S.; Bittner, E. R.; Baumgarten, M. *J. Chem. Phys.* **2001**, *114*, 5863–5870.

It has recently been suggested that, in contrast to C–C stretch relaxations, such dynamic planarization causes an extension of the excitonic wave function.¹⁰ A clear analysis of these two counteracting effects is challenging since they are expected to occur over a range of time scales resulting in an overall complex evolution of the excited-state wavefunction with time. However, a better understanding of the time-dependent nature of the excited state is urgently required as it has a strong influence on exciton diffusivity and charge carrier mobility,¹¹ which in turn has a direct impact on the optoelectronic properties.

In the study presented here, we draw a clear distinction between the effects of C–C stretch and inter-ring torsional relaxation on the electronic delocalization of the excited state for a set of conjugated oligomers. For this purpose, we investigated conjugated zinc porphyrin oligomers, for which we were able to gain accurate control over the molecular backbone conformation and the presence of a torsional degree of freedom between porphyrin units. Conjugated porphyrin oligomers present an ideal choice for a study of this kind, because they allow assembly into a chosen geometry through coordination between their metal cores and purpose-made templates.^{12–14} Similar porphyrin architectures have been exploited by nature over a great length of time in processes such as oxygen transport or photosynthesis,¹⁵ inspiring work on the synthetic generation of artificial light-harvesting systems by use of metal coordination.^{16–18} The molecules under investigation here comprise zinc porphyrin macrocycles that are linked through butadiyne bridges into conjugated oligomers. The lowest electronic transition is polarized in the direction of the long axis of the molecule and generates an excited-state wave function that is delocalized to a certain extent along the backbone of the molecule.^{19–22} These materials are therefore comparable to typical conjugated oligomers, such as oligo(phenylene vinylenes), oligothiophenes, or oligofluorenes, that also display degrees of freedom for both C–C stretch and inter-ring torsional vibrations.^{7,9} By use of metal-coordinating templates that induce a different extent of bending on the oligomer backbone we are able to show that the initially generated exciton is highly delocalized but contracts rapidly on the 100 fs time scale as a result of geometric relaxation, most likely along the C–C stretch coordinate.

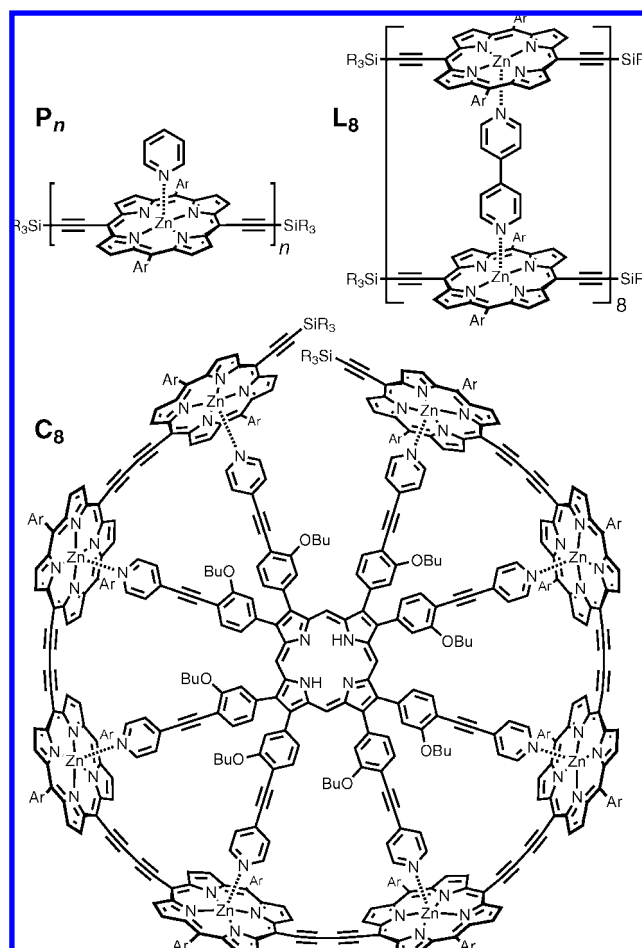


Figure 1. Chemical structures of the butadiyne-linked zinc porphyrin assemblies under investigation: (P_n) single-stranded porphyrin oligomers with $n = 4, 6, 8$, (L_8) double-stranded ladder octamer, and (C_8) cyclic octamer complex (Ar = 3,5-dioctyloxyphenyl; R = hexyl).

Through a choice of templates that either allow or suppress interporphyrin torsional motions we are able to compare the influence of these on the further evolution of the excitonic state. We find that inter-ring torsional relaxation leads to a planarization of the molecular backbone on the 100 ps time scale that is accompanied by an increase in both the oscillator strength and the extent of the excitonic wave function. These results clearly demonstrate that the extent of the excited-state electronic delocalization in conjugated oligomers oscillates over time, in accordance with the nature of the vibrational modes involved in the electronic transition.

Experimental Section

Materials. Figure 1 illustrates the chemical structure of the porphyrin complexes under investigation. The syntheses and structural characterization of these compounds have already been described in detail elsewhere.^{12–14,23} For further information on structural studies carried out on these compounds the reader is therefore referred to the attached Supporting Information and the references provided therein. The butadiyne-linked zinc porphyrin oligomers (P_n , where $n = 4, 6, 8$) were dissolved in toluene (concentration $\sim 1 \times 10^{-4}$ M) in the presence of 1% (by volume fraction) pyridine to prevent aggregation and allow the photophysi-

- (10) Westenhoff, S.; Beenken, W. J. D.; Friend, R. H.; Greenham, N. C.; Yartsev, A.; Sundstrom, V. *Phys. Rev. Lett.* **2006**, *97*, 166804.
- (11) Beljonne, D.; Hennebicq, E.; Daniel, C.; Herz, L. M.; Silva, C.; Scholes, G. D.; Hoeben, F. J. M.; Jonkheijm, P.; Schenning, A. P. H. J.; Meskers, S. C. J.; Phillips, R. T.; Friend, R. H.; Meijer, E. W. *J. Phys. Chem. B* **2005**, *109*, 10594–10604.
- (12) Hoffmann, M.; Wilson, C. J.; Odell, B.; Anderson, H. L. *Angew. Chem., Int. Ed.* **2007**, *46*, 3122–3125.
- (13) Screen, T. E. O.; Thorne, J. R. G.; Denning, R. G.; Bucknall, D. G.; Anderson, H. L. *J. Am. Chem. Soc.* **2002**, *124*, 9712–9713.
- (14) Screen, T. E. O.; Thorne, J. R. G.; Denning, R. G.; Bucknall, D. G.; Anderson, H. L. *J. Mater. Chem.* **2003**, *13*, 2796–2808.
- (15) McDermott, G.; Prince, S. M.; Freer, A. A.; Hawthornthwaite-Lawless, A. M.; Papiz, M. Z.; Cogdell, R. J.; Isaacs, N. W. *Nature* **1995**, *374*, 517–521.
- (16) Nakamura, Y.; Aratani, N.; Osuka, A. *Chem. Soc. Rev.* **2007**, *36*, 831–845.
- (17) Kobuke, Y. *Eur. J. Inorg. Chem.* **2006**, 2333–2351.
- (18) Kelley, R. F.; Goldsmith, R. H.; Wasielewski, M. R. *J. Am. Chem. Soc.* **2007**, *129*, 6384–6385.
- (19) Beljonne, D.; O’Keefe, G. E.; Hamer, P. J.; Friend, R. H.; Anderson, H. L.; Brédas, J. L. *J. Chem. Phys.* **1997**, *106*, 9439–9460.
- (20) Stranger, R.; McGrady, J. E.; Arnold, D. P.; Lane, I.; Heath, G. A. *Inorg. Chem.* **1996**, *35*, 7791–7797.
- (21) Anderson, H. L. *Chem. Commun.* **1999**, 2323–2330.
- (22) Drobizhev, M.; Stepanenko, Y.; Dzenis, Y.; Karotki, A.; Rebane, A.; Taylor, P. N.; Anderson, H. L. *J. Phys. Chem. B* **2005**, *109*, 7223–7236.

- (23) Drobizhev, M.; Stepanenko, Y.; Rebane, A.; Wilson, C. J.; Screen, T. E. O.; Anderson, H. L. *J. Am. Chem. Soc.* **2006**, *128*, 12432–12433.

cal properties of isolated oligomers to be examined.²⁴ Double-strand ladder octamer (L_8) was self-assembled by mixing linear octamer with 4,4'-bipyridyl (Bipy) at a ratio of 1:4 in toluene at an octamer concentration of $\sim 1 \times 10^{-4}$ M. It has recently been demonstrated^{13,14} that titration of P_n with an increasing fraction of Bipy initially leads to the breaking up of aggregated oligoporphyrins and the formation of double-strand ladders as indicated in Figure 1. At even higher Bipy concentration, oligoporphyrin single strands are formed, and the near-IR (NIR) absorption spectra approach those of P_n in the presence of pyridine. For the present study, the Bipy fraction was carefully set to ensure the predominant presence of the double-stranded ladder octamer complex L_8 . Cyclic porphyrin octamer complex (C_8) was produced by complexation of a porphyrin octamer P_n with a complementary octadentate template (Figure 1) at a ratio of 1:1 in toluene (octamer concentration $\sim 1 \times 10^{-4}$ M) as described in detail recently.¹² UV–NIR absorption spectra were taken with a spectrophotometer (Perkin-Elmer, Lambda 9) for all solutions to ensure the presence of the desired porphyrin complexes during the measurements.

Femtosecond Photoluminescence Experiments. To study the photoexcitation dynamics of the complexes, time-resolved photoluminescence (PL) measurements were conducted using the up-conversion (PL UC) technique²⁵ on solutions held in a quartz cuvette. Samples were excited with the output of a mode-locked Ti:Sapphire laser (Spectra Physics Tsunami) providing pulses of 100 fs duration at a photon energy of 1.61 eV (770 nm) and a repetition rate of 80 MHz. The emerging photoluminescence was collected by a pair of off-axis parabolic mirrors and focused onto a β -barium borate (BBO) crystal mounted on a rotation stage to allow tuning of the phase-matching angle. The collection direction was set at right angle to the excitation beam, which entered the cell close to its front surface in order to avoid artifacts arising from self-absorption. An intense vertically polarized gate beam (photon energy 1.61 eV) arriving at the BBO crystal at adjustable time delays was used to up-convert the PL at given times after excitation. The resulting sum-frequency photons were collected, dispersed in a monochromator (Jobin Ivon Triax 190), and detected by a liquid-nitrogen-cooled CCD. Only the vertical polarization component of the PL was up-converted in this setup; therefore, either the parallel or perpendicular luminescence polarization with respect to the excitation polarization was selected by changing the polarization of the excitation beam through rotation of a half-wave plate and a Glan–Thompson polarizer. The PL anisotropy was calculated from these PL intensity components as $\gamma = (I_{\parallel} - I_{\perp}) / (I_{\parallel} + 2I_{\perp})$. The overall time resolution of the system was predominantly limited by the size of the imaged excitation spot in the solution to 800 fs. The vertically polarized component of the time-integrated photoluminescence (TI PL) was measured by using the same spectrometer and replacing the BBO crystal with a Glan–Thompson polarizer. Both time-integrated and time-resolved spectra were corrected for instrumental response using a filament lamp of known emissivity.

Results and Discussion

Exciton Delocalization and Self-Trapping in Butadiyne-Bridged Porphyrin Oligomers. Figure 2 displays the absorption and emission spectra for butadiyne-bridged porphyrin tetramer P_4 , hexamer P_6 , and octamer P_8 . The lowest absorption band is spectrally broad and shifts to the red with increasing oligomer length, while the emission is considerably narrower than the absorption. The changes in the nature of the electronic transitions with oligomer length are in general agreement with those

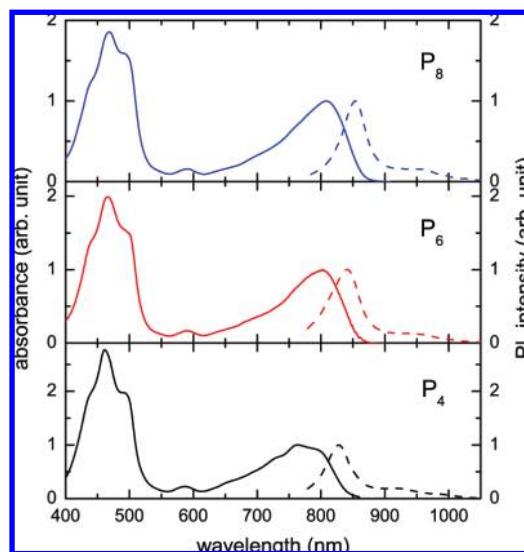


Figure 2. Absorption (solid line) and time-integrated emission (dotted line) spectra for single-stranded porphyrin octamers P_8 (top), hexamer P_6 (middle), and tetramer P_4 (bottom) in toluene containing 1% pyridine. The emission was recorded after excitation at 770 nm (1.61 eV).

observed previously for alkyne-linked porphyrins.^{24,26–29} Unsubstituted zinc porphyrin monomers display an intense $S_0 \rightarrow S_2$ transition at ~ 400 nm (the Soret or B-band) and a weaker $S_0 \rightarrow S_1$ transition at ~ 550 nm (the Q-band).²¹ Linking of more than one porphyrin unit through an alkyne bridge lifts the fourfold symmetry of the monomer and lead to a splitting of B- and Q-band transitions into two components each, which are polarized parallel (x) and perpendicular (y) to the direction defined by the long axis of the oligomer.^{19,22,30} As shown in Figure 2, with increasing oligomer length the lowest transition band Q_x (around 800 nm) shifts to the red and intensifies with respect to the B-band.^{24,28} Previous studies have demonstrated that the extent of such changes depends sensitively on the length of the bridge and its attachment position on the porphyrin periphery^{27,30} (e.g., meso or β). Both parameters influence the extent to which the porphyrin electronic wave functions are perturbed and impose steric constraints on the dihedral angle between adjacent porphyrin units. For the meso-to-meso butadiyne-bridged dimer belonging to the family of oligomers investigated here, theoretical calculations^{19,31} have indicated that the observed Soret band splitting is too large to be adequately described by the simple point–dipole exciton coupling theory developed by Kasha et al.³² These calculations imply that significant electronic overlap exists between the porphyrin macrocycles leading to enhanced conjugation with increasing length of the molecular backbone in accordance with a preference toward a planar structure. Accordingly, theoretical studies have indicated that the ground-state potential for torsional motion of porphyrins about the axis of the butadiyne bridge

(24) Winters, M. U.; Kärnbratt, J.; Eng, M.; Wilson, C. J.; Anderson, H. L.; Albinsson, B. *J. Phys. Chem. C* **2007**, *111*, 7192–7199.

(25) Chang, M. H.; Hoeben, F. J. M.; Jonkheijm, P.; Schenning, A. P. H. J.; Meijer, E. W.; Silva, C.; Herz, L. M. *Chem. Phys. Lett.* **2006**, *418*, 196–201.

(26) Anderson, H. L.; Martin, S. J.; Bradley, D. D. C. *Angew. Chem., Int. Ed. Engl.* **1994**, *33*, 655–657.

(27) Lin, V. S. Y.; Therien, M. J. *Chem.—Eur. J.* **1995**, *1*, 645–651.

(28) Duncan, T. V.; Susumu, K.; Sinks, L. E.; Therien, M. J. *J. Am. Chem. Soc.* **2006**, *128*, 9000–9001.

(29) Taylor, P. N.; Huuskonen, J.; Rumbles, G.; Aplin, R. T.; Williams, E.; Anderson, H. L. *Chem. Commun.* **1998**, 909–910.

(30) Kumble, R.; Palese, S.; Lin, V. S. Y.; Therien, M. J.; Hochstrasser, R. M. *J. Am. Chem. Soc.* **1998**, *120*, 11489–11498.

(31) Anderson, H. L. *Inorg. Chem.* **1994**, *33*, 972–981.

(32) Kasha, M.; Rawls, H. R.; El-Bayoumi, M. A. *Pure Appl. Chem.* **1965**, *11*, 371.

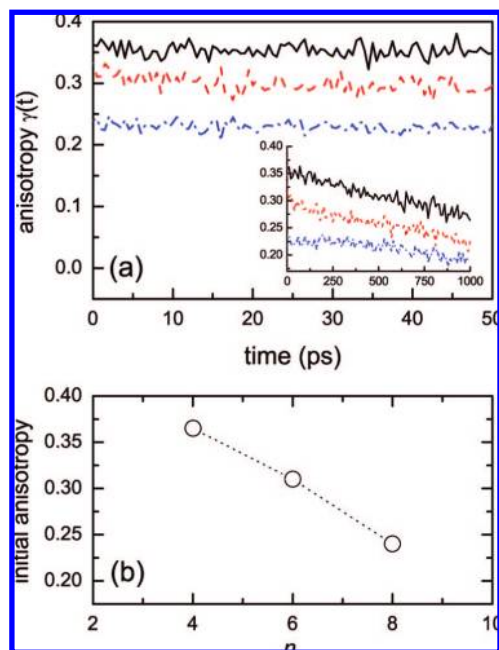


Figure 3. (a) PL polarization anisotropy as a function of time after excitation at 770 nm (1.61 eV) and detection at 850 nm (1.46 eV) for the single-stranded zinc porphyrin tetramer P_4 (solid line), hexamer P_6 (dashed line), and octamer P_8 (dotted line). The inset shows the behavior over the first nanosecond after excitation. Variation of the detection wavelength across the Q_x emission band resulted in anisotropy transients that were identical within the accuracy of the measurements (ref 48). (b) Initial PL polarization anisotropy as a function of the number of repeat units n comprising the single-stranded porphyrin oligomers P_n .

has a relatively shallow minimum centered at zero dihedral angle, with various theoretical methods^{20,24,27} yielding estimates for the barrier height for full rotation between 0.7 and 15 kcal mol⁻¹. Quantum chemical calculations indicate that the excited state, on the other hand, has a significant cumulenlic character with the optimized geometry displaying a lengthening of triple bonds and a shortening of single bonds on the butadiyne bridge.¹⁹ The resulting delocalization of the highest occupied molecular orbital (HOMO) level over the whole porphyrin oligomer is thus expected to cause a red-shift and intensification of the Q_x transition¹⁹ and a further planarization of the molecular structure resulting from a steeper potential for interporphyrin torsions in the S_1 state.²⁴ Similar effects are common for many conjugated oligomers with ring torsional degrees of freedom, such as oligo(phenylene vinylenes) and oligo(phenylenes).^{6,7,9,33} For these molecules, excitation was theoretically shown to induce changes in the torsional potential (and the resulting torsional disorder)³³ and a redistribution from stiff bond-stretch vibrational to softer torsional accepting modes.⁹ These mechanisms were evoked to explain the observed spectrally broadened absorption and significantly narrower emission for these materials. The occurrence of similar effects for butadiyne-linked porphyrins (see Figure 2) makes these oligomers ideal model systems for the investigation of electronic delocalization and geometric relaxation effects in extended conjugated molecules.

Figure 3a shows the temporal dependence of the PL anisotropy $\gamma(t)$ for the three porphyrin oligomers within the first 50 ps after excitation. The emitted PL does not depolarize to any observable extent, suggesting that reorientation of the emitting transition dipole moment is absent over this time interval.

Surprisingly, the initial PL anisotropy value $\gamma(0)$ clearly decreases with increasing oligomer length. Previous studies for unsubstituted magnesium porphyrin monomers, whose fourfold symmetry leads to a degeneracy of the Q_x and Q_y transitions, have shown that simultaneous excitation of both states results in an initially high anisotropy of ~ 0.7 , followed by a rapid decay to ~ 0.1 within ~ 1 ps caused by dephasing between the two states.³⁴ However, in alkyne-linked porphyrin oligomers the splitting between the Q_x and Q_y transitions means that selective excitation of Q_x should create an excited state with a well-defined transition dipole moment oriented along the long axis of the molecule resulting in an expected initial PL anisotropy of $\gamma(0) = 0.4$ in the absence of other depolarizing mechanisms.³⁵ Values of similar magnitude ($\gamma(0) \sim 0.38\text{--}0.4$) have been observed experimentally for ethynyl-bridged zinc porphyrin dimers^{30,36} upon direct excitation of the Q_x -band. For the oligomers under investigation here, only the shortest (P_4) shows a comparable initial anisotropy value of $\gamma(0) \sim 0.37$ suggesting that the longer oligomers are subject to an ultrafast PL depolarization that occurs well within the time resolution of our system (800 fs). An ultrafast interconversion between states following unintentional excitation of the orthogonally polarized Q_y transition can be ruled out as its transition energy of 2.1 eV (590 nm—see Figure 2) is substantially higher than that of the excitation pulse (1.6 eV). However, a possible mechanism for the observed depolarization may be exciton self-trapping following ultrafast vibrational relaxation of the excited molecule. It has recently been proposed that such effects may be responsible for the ultrafast (<100 fs) PL depolarization observed for poly(phenylene vinylene) derivatives in solution.⁸ Theoretical simulations of the lowest electronic transition moments for conjugated thiophene oligomers have indicated that the formation of fully delocalized excitonic states may be possible even in the presence of certain types of kinks and torsions on the molecular backbone.³⁷ However, it was proposed that the subsequent geometric relaxation toward the potential minimum of the C—C stretching mode ($\bar{\nu}_{C-C} \approx 1300$ cm⁻¹) may lead to a dynamic localization of the relaxed excited state on the lower-energy segment of the molecule partitioned by the defect. For a bent segment, this process will then be accompanied by a reorientation of the transition dipole moment on the time scale of the vibrational period (~ 25 fs).³⁷ Theoretical calculations suggest that such exciton self-trapping effects are likely to be less pronounced for shorter conjugated oligomers, for which the excitonic wave functions are already relatively confined prior to geometric relaxation of the molecule.⁷ The recent observation that the extent of ultrafast PL depolarization is reduced with decreasing average conjugation length for isolated chains of a conjugated poly(phenylene vinylene) derivative has therefore been attributed to exciton self-trapping on wormlike chains.⁸ However, for conjugated polymers a detailed analysis is complicated by the distribution of conjugated segments with varying lengths that typically make up a single chain. For the butadiyne-linked porphyrins under investigation here, we are able to demonstrate a clear correlation between oligomer length and the extent to which an initial ultrafast PL

(33) Beenken, W. J. D.; Lischka, H. *J. Chem. Phys.* **2005**, *123*, 144311.

(34) Galli, C.; Wynne, K.; Lecours, S. M.; Therien, M. J.; Hochstrasser, R. M. *Chem. Phys. Lett.* **1993**, *206*, 493–499.

(35) Valeur, B. *Molecular Fluorescence: Principles and Applications*; Wiley-VCH: Weinheim, Germany, 2002.

(36) Rubtsov, I. V.; Susumu, K.; Rubtsov, G. I.; Therien, M. J. *J. Am. Chem. Soc.* **2003**, *125*, 2687–2696.

(37) Beenken, W. J. D.; Pullerits, T. *J. Phys. Chem. B* **2004**, *108*, 6164–6169.

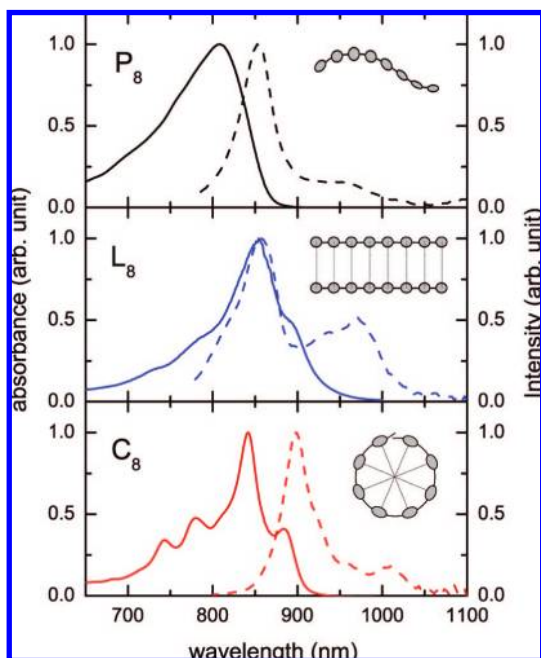


Figure 4. Absorption (solid line) and time-integrated emission (dashed line) spectra for the single-stranded porphyrin octamer P_8 (top), the double-stranded ladder octamer L_8 (middle), and the cyclic octamer C_8 (bottom). The emission was recorded after excitation at 770 nm (1.61 eV).

depolarization occurs: for the tetramer an initial PL anisotropy of 0.37 is observed, which falls to 0.24 for the octamer—see Figure 3b. These results strongly suggest dynamic exciton self-trapping on porphyrin oligomers that adopt a wormlike conformation in solution as the most likely mechanism for the observed depolarization effects. To examine this hypothesis, further experiments were conducted on porphyrin oligomers for which the backbone had been forced into specific geometries through coordination with selected templates, as discussed in the following section.

For longer times after excitation, the PL polarization anisotropy decays with time constants of ~ 3 – 5 ns depending on oligomer length (see the inset to Figure 3a). These dynamics occur on the time scale of molecular reorientation in the solution in agreement with previous reports of somewhat smaller time constants (few hundred picoseconds) observed for shorter, but otherwise similar, porphyrin oligomers.^{30,34,38}

Influence of Backbone Conformation on the Ultrafast PL Depolarization in Porphyrin Octamers. To investigate further the origin of the dynamic depolarization effects described in the previous section, measurements were conducted on porphyrin octamers adopting the three different backbone geometries indicated in Figure 1. The absorption and time-integrated emission spectra are shown in Figure 4 for wormlike isolated octamers (P_8), double-strand octamer ladders (L_8), and cyclic octamer assemblies (C_8). A detailed analysis of the spectral features is complicated by the presence of a multitude of closely spaced electronic transitions in these materials,¹⁹ but some general trends can be observed. First, coordination of the octamer with a Bipy or octadentate template leads to a red-shift in the absorption and a considerable sharpening of the emission features. Second, the Stokes shift between absorption and emission is reduced from ~ 45 nm (80 meV) to ~ 3 nm

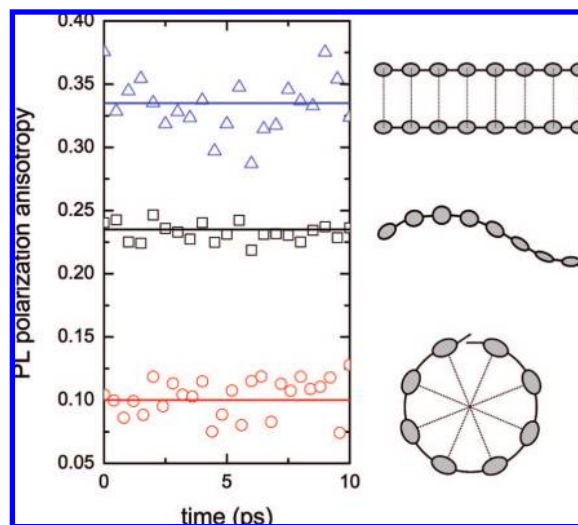


Figure 5. PL polarization anisotropy as a function of time after excitation at 770 nm for the single-stranded porphyrin octamer P_8 (squares, detection at 850 nm), the double-stranded ladder octamer L_8 (triangles, detection at 900 nm), and the cyclic octamer C_8 (circles, detection at 900 nm). Variation of the detection wavelength across the Q_x emission band resulted in anisotropy transients that were identical within the accuracy of the measurements (ref 48).

(6 meV) when moving from the single-stranded (P_8) to the double-stranded (L_8) octamers. These observations indicate that upon coordination with the template, interporphyrin torsional motion is suppressed, leading to the formation of rigid straight (L_8) or cyclic (C_8) structures and an extension of the effective π -conjugation length. Previous characterization of such assemblies using small-angle neutron scattering^{13,14} has shown that long ($n \sim 10$ – 15) butadiyne-linked porphyrin oligomers adopt a rodlike structure in solution that extends by a factor of ~ 1.5 in length upon formation of double-stranded ladders. Similarly, a study of the cross sections for two-photon absorption in these oligomers showed that the “conjugation signature” or effective electronic delocalization in the single-strand conformation only encompasses a fraction of the full length, in particular for the longer oligomers.²³ In contrast, formation of double-strand ladders was shown to lead to a significant increase of the effective conjugation length, again in particular for the longer oligomers. Taken together, these observations demonstrate that in solution, the single-stranded P_8 can be considered as a wormlike object, whereas the double-stranded L_8 and the cyclic C_8 form extended objects with near-zero angle between adjacent porphyrin units.

Figure 5 shows the time-resolved PL polarization anisotropy over the first 10 ps after excitation for the octamer adopting the three different conformations. Again, the anisotropy is static over this time scale for all three cases but assumes different values: upon formation of a double-stranded ladder, $\gamma(0)$ increases to a value of ~ 0.34 from the significantly lower value of ~ 0.24 for the wormlike single-stranded octamer. These measurements are clear evidence that the observed ultrafast PL depolarization indeed originates from exciton self-trapping: although the reorientation of the transition dipole moment with geometric relaxation may be possible in wormlike bent or kinked single-stranded conformations, a forced planarization of the molecular backbone will inhibit such reorientation. However, to distinguish clearly between effects caused by a bend in the overall backbone geometry and those resulting from a suppression of torsional motion between adjacent porphyrin units, the

(38) Maiti, N. C.; Mazumdar, S.; Periasamy, N. *J. Phys. Chem.* **1995**, *99*, 10708–10715.

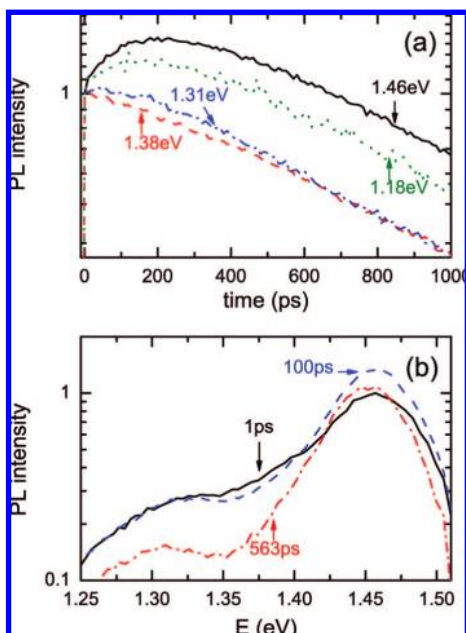


Figure 6. PL emission dynamics for the single-stranded zinc porphyrin octamer P_8 . (a) PL decay transients detected at 1.46 eV or 850 nm (solid line), 1.38 eV or 900 nm (dashed line), 1.31 eV or 950 nm (dash-dotted line), and 1.18 eV or 1050 nm (dotted line). (b) Time-resolved PL spectra detected at 1 (solid line), 100 (dashed line), and 563 ps (dash-dotted line) after photoexcitation.

cyclic octamer was also investigated (see Figure 5). For C_8 the backbone should be more strongly curved than for the wormlike P_8 , and a lower initial anisotropy is indeed observed. The observed value of 0.1 is as would be expected for a complete depolarization of the transition dipole moment within the two-dimensional plane of the template. It is important to note that the mechanism for this depolarization is fundamentally different for that observed in unsubstituted zinc porphyrin monomers, for which it is caused by dephasing between two degenerate, orthogonally polarized states. Our combined observations show that for the cyclic octamer, the ultrafast PL depolarization is instead the result of an initial electronic delocalization that extends almost over the entire length of the molecular backbone but may subsequently self-localize following geometric relaxation. This situation is reminiscent of that for natural light-harvesting systems in purple photosynthetic bacteria that incorporate cyclic assemblies bacteriochlorophyll *a* chromophores that are either monomeric (B800 complex) or tightly coupled 18-mers or 16-mers (B850 complexes).¹⁵ For some of the more strongly coupled natural porphyrin ring assemblies, fluorescence depolarization has been observed to occur on the time scale of a few hundred femtoseconds after excitation,³⁹ and theoretical simulations have indicated that, while immediately after generation the exciton wave packet is delocalized over a substantial portion of the ring, it contracts to a much smaller size within a few hundred femtoseconds.⁴⁰ For these natural light-harvesting systems such strong electronic coupling between porphyrin monomers is facilitated by an ingenious mixture of a favorable assembly geometry and a hydrophobic environment that reduces the dielectric constant.¹⁵ In contrast, the synthetic cyclic porphyrin C_8 under investigation

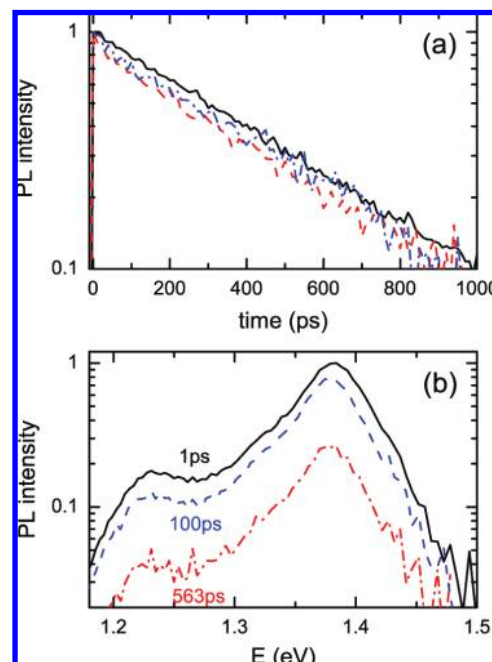


Figure 7. PL emission dynamics for the cyclic zinc porphyrin octamer C_8 . (a) PL decay transients detected at 1.38 eV or 900 nm (solid line), 1.31 eV or 950 nm (dashed line), and 1.18 eV or 1050 nm (dash-dotted line). (b) Time-resolved PL spectra detected at 1 (solid line), 100 (dashed line), and 563 ps (dash-dotted line) after photoexcitation.

here induces a full initial excitonic delocalization by the use of conjugated bridges between the porphyrin subunits.

Effect of Torsional Relaxation on the Photoexcitation Dynamics of Butadiyne-Bridged Porphyrin Octamers. The excitonic self-localization effects described in the previous section occur on the subpicosecond time scale and are therefore probably associated with fast vibrational relaxation along the C–C stretching coordinates of the porphyrin units and the linking bridges. However, torsional relaxation of the porphyrin oligomers is also likely to play a role, albeit on longer time scales.^{24,36} To investigate such effects, the emission within the first nanosecond after excitation was measured for the single-strand octamer P_8 and compared to that of the cyclic octamer C_8 , which also has a bent molecular backbone but lacks the torsional degree of freedom (see Figures 6 and 7). For the flexible single-strand octamer, excitation just above the peak of the Q_x absorption band results in complex decay dynamics that depend on the spectral position at which they were recorded (Figure 6a). Near the center of the main peak (1.46 eV) the emission displays a slow secondary rise that reaches a maximum at 200 ps after excitation. To the low-energy side of the peak this rise is less pronounced and followed by a monotonic decay over the next few hundred picoseconds. In comparison, the PL decay dynamics for the torsionally rigid cyclic octamer (Figure 7a) are independent of the detection energy and display a monoexponential decay with a time constant of ~ 420 ps. Accordingly, the measured time-resolved spectra (Figure 7b) do not change shape over the first few hundred picoseconds and are spectrally identical to the time-integrated PL spectrum. The complex emission dynamics observed for the single-stranded octamer P_8 must therefore be linked to its freedom for torsional motion between adjacent porphyrin units. To allow a more detailed analysis of these relaxation dynamics, the emission spectra of P_8 at a range of times after excitation were fitted with the sum of three Gaussians, the first of which was

(39) Bradforth, S. E.; Jimenez, R.; Mourik, F. v.; Grondelle, R. v.; Flemming, G. R. *J. Phys. Chem.* **1995**, *99*, 16179–16191.

(40) Dahlbom, M.; Pullerits, T.; Mukamel, S.; Sundström, V. *J. Phys. Chem. B* **2001**, *105*, 5515–5524.

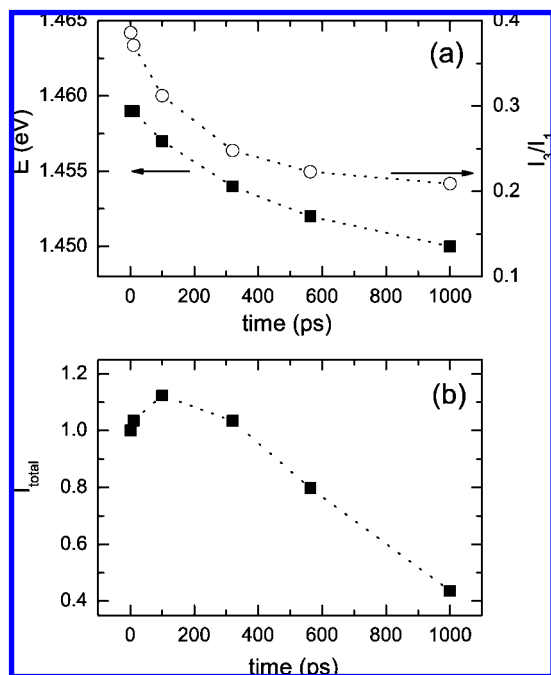


Figure 8. Analysis of the PL emission dynamics for the single-stranded zinc porphyrin octamer. (a) Parameters extracted from Gaussian fits to the time-resolved PL spectra shown in Figure 6b according to the procedure described in the text. The solid squares indicate the energy of the main emission peak, and the open circles represent the ratio of the spectrally integrated emission intensity of the peak located 150 meV below the main peak, I_3 , to that of the main peak I_1 . (b) Total PL emission intensity calculated from the data displayed in Figure 6b through integration over the shown spectral range.

used to fit the main transition near 1.46 eV, and the other two were set at energies of 74 and 150 meV below the main peak. It was found that two Gaussians were needed for a satisfactory fit of the low-energy tail of the emission—the origin of these features will be discussed in more detail below. The amplitude of each of the three Gaussians was allowed to fluctuate freely for the fits, while the widths were fixed at values between 0.08 and 0.12 meV. Figure 8a shows some of the relevant parameters extracted from these fits as a function of time after excitation. The energy of the main emission peak E_1 (and its low-energy tail) is found to decrease by ~ 10 meV over the first nanosecond. At the same time, the ratio of the spectrally integrated emission intensity of the peak located 150 meV below the main peak to that of the main peak (I_3/I_1) decreases from ~ 0.4 to ~ 0.2 . A similar behavior is observed for the peak located 74 meV below the main peak, for which the ratio decreases from $I_2/I_1 \sim 0.25$ to ~ 0.1 (not shown). As a third indicator, the overall emission intensity I_{total} was extracted from the time-resolved spectra through integration and displayed in Figure 8b. A secondary rise of I_{total} is found that matches the time scale of the main changes occurring in E_1 and I_3/I_1 , after which the total emission decays monotonically as a result of radiative and nonradiative recombination.

Recently, femtosecond transient absorption measurements on meso-to-meso ethyne-bridged porphyrin dimers have shown that excitation just above the Q_x transition energy results in a red-shift and monotonic decay of the $S_0 \rightarrow S_1$ photobleach that is accompanied by an increase in the intensity of the $S_1 \rightarrow S_n$ photoinduced absorption over the first 100 ps.³⁶ It was suggested that these changes are caused by the structural relaxation associated with the planarization of the molecular backbone

following excitation of a dimer ensemble with a wide distribution of torsional angles between adjacent porphyrins. Our comparison of the time-resolved emission spectra for butadiyne-linked porphyrin octamers with and without the torsional degree of freedom demonstrates unambiguously that such effects are indeed linked to torsional geometric relaxation of the molecule. In addition, the use of time-resolved emission spectroscopy enables us to probe directly the evolution of the Q_x excited state during torsional relaxation. The three parameters extracted from the emission spectra and displayed in Figure 8 each independently indicate that the torsional relaxation of the octamer is accompanied by an enhancement of conjugation and an increase in excitonic delocalization over the first ~ 100 ps. The increase in the overall emission intensity suggests a growth in the oscillator strength, whereas the red-shift in the emission band is indicative of an increasing electronic delocalization of the excited state. The change in intensity ratio between the main and the lower-energy emission peaks, however, needs more careful consideration. The spacing of these sub-bands with respect to the main peak has prompted previous investigators to assign these peaks to phonon replica.^{19,41} A large number of peaks in the resonance Raman spectra has in fact been observed with vibrational energies between 500 and 1600 cm^{-1} (60–200 meV) for zinc porphyrin monomers^{19,41} and butadiyne-linked dimers.¹⁹ A study of the ground-state and excited-state vibrational structures of zinc porphyrin monomers using picosecond resonance Raman spectroscopy concluded that very small geometric distortions occur after excitation of the monomer so that the vibronic replica have to be considered in terms of mode mixing (Herzberg–Teller coupling) rather than a Franck–Condon mechanism.⁴¹ However, for the butadiyne-bridged oligomers the situation may be substantially different: theoretical calculations^{19,24} and the experimental results presented here and elsewhere^{24,30} strongly suggest that both fast (e.g., C–C stretch) vibrations and slow interporphyrin torsions couple effectively to the electronic transitions of the energetically lowest transitions in butadiyne-linked porphyrin oligomers. In this case, the emission peak ratio I_3/I_1 displayed in Figure 8a may be interpreted as the Huang–Rhys factor for the Franck–Condon progression for the vibration mode at 150 meV (1200 cm^{-1}), which most likely originates from C–C stretch vibrations along the porphyrin rings and linking butadiyne bridges. Joint experimental and theoretical analysis of *p*-phenylenevinylene oligomers have shown that the Huang–Rhys factor for structural relaxation along the C–C stretch coordinate decreases with increasing oligomer length.^{6,7} In this sense, the decrease in I_3/I_1 observed for the butadiyne-linked porphyrin octamer may also be interpreted as indicative of an increase in conjugation and excited-state electronic delocalization.

For the conjugated porphyrin oligomer under investigation here, torsional relaxation appears to be completed approximately within the first 200 ps after excitation. Slow vibrational cooling effects have been studied for a range of other conjugated oligomers with C–C stretch vibrational and inter-ring torsional degrees of freedom, such as polythiophene^{10,42} and polyfluorene⁴³ derivatives. Torsional relaxation times ranging between tens and hundreds of picoseconds are typically observed, which

(41) Kumble, R.; Loppnov, G. R.; Hu, S. Z.; Mukherjee, A.; Thompson, M. A.; Spiro, T. G. *J. Phys. Chem.* **1995**, *99*, 5809–5816.

(42) Westenhoff, S.; Beenken, W. J. D.; Yartsev, A.; Greenham, N. C. *J. Chem. Phys.* **2006**, *125*, 154903.

(43) Hintschich, S. I.; Dias, F. B.; Monkman, A. P. *Phys. Rev. B* **2006**, *74*, 045210.

depend critically on the oligomer length, solvent viscosity, and temperature.⁴³ Theoretical modeling of such picosecond vibrational cooling effects for small molecules have employed simple models of vibrational energy transfer from hot solute molecules to the neighboring solvent shell, followed by dissipation of energy within the solvent.⁴⁴ Our results indicate the need for further development of adequate models for dynamic geometric relaxation processes in much larger conjugated oligomers with electronic transitions that couple strongly to both vibrational and torsional modes.

Conclusions

Upon excitation, conjugated oligomers typically display geometric relaxation along a range of configuration coordinates. These changes lead to complex dynamics in the electronic delocalization of the excited state and the nature of the transition dipole moment over a range of different time scales. In the study presented here, we have been able to distinguish clearly between the two modes that preferentially couple to the electronic transitions in these systems, i.e., carbon–carbon bond stretching and inter-ring torsional vibrations. For this purpose, we exploited the remarkable potential of conjugated porphyrins for supramolecular assembly, which allows porphyrin oligomers to be prepared in a chosen backbone geometry and with or without an interporphyrin torsional degree of freedom. Our results demonstrate that excitation of the conjugated porphyrin oligomers initially prepares an excitonic state that is delocalized along most of the conjugated molecule. Geometric relaxation involving fast stretching modes then leads to a decrease in the extent of the excited-state wave function, or “exciton self-trapping” on a subpicosecond time scale, as indicated by the ultrafast emission depolarization for bent conjugated oligomers. Subsequently, changes in the interporphyrin torsional potential force the molecular backbone to evolve into a more planar geometry over the next few tens or hundreds of picoseconds. The observed energetic shifts and changes in the emission shape and intensity strongly suggest that over this time scale the effective conjugation length and excitonic delocalization along the porphyrin oligomer backbone increases again. It has recently been shown that such a secondary increase in excitonic delocalization length over a the first few tens of picoseconds has to be assumed in order to provide an accurate model of the energetic relaxation associated with planarization of a polythiophene derivative in

solution.¹⁰ Taken together, our results therefore indicate that the extent of the excitonic delocalization along the conjugated backbone oscillates after excitation in accordance with the time scales of the vibrational modes coupled to the transition. Theoretical studies that are able to incorporate such complex vibronic dynamics are urgently needed in order to provide a more comprehensive picture of how exactly the nature of the excited electronic states evolves over their lifetime.

Our experimental study presents a picture of the dynamic delocalization of the exciton along a conjugated oligomer backbone in solution. However, the implications of this work are of a more general nature: a recent study of the microwave-frequency mobility for positive charge carriers on porphyrin oligomers identical to those investigated here showed that ladder formation increased the mobility by an order of magnitude with respect to that for the single strand.⁴⁵ While it is currently unclear whether these changes result from suppression of inter-ring torsional motion or a linearization of the molecular backbone, the results suggest that electronic delocalization effects similar to those described for excitons here may also be of relevance to charge motion. Finally, the scenario may be different for conjugated segments in close proximity in solution or as part of a solid phase. Here, torsional motion may be partly suppressed¹⁰ and the excitonic wave function may also initially be delocalized across more than one conjugated oligomer or polymer chain segment.^{11,46,47}

Acknowledgment. Financial support for this work was provided by the Engineering and Physical Sciences Research Council (U.K.).

Supporting Information Available: Characterization details of the porphyrin complexes under investigation. This material is available free of charge via the Internet at <http://pubs.acs.org>.

JA711222C

(45) Grozema, F. C.; Houarner-Rassin, C.; Prins, P.; Siebbeles, L. D. A.; Anderson, H. L. *J. Am. Chem. Soc.* **2007**, *129*, 13370–13371.

(46) Yang, X. J.; Dykstra, T. E.; Scholes, G. D. *Phys. Rev. B* **2005**, *71*, 045203.

(47) Chang, M. H.; Frampton, M. J.; Anderson, H. L.; Herz, L. M. *Phys. Rev. Lett.* **2007**, *98*, 027402.

(48) To investigate the dependence of the PL polarization anisotropy measurements on detection wavelength across the Q_x emission band, curves were recorded at 840, 850, 900, and 950 nm for P_4 , 850 and 900 nm for P_6 , 850, 900, and 1050 nm for P_8 , and 900 and 1050 nm for C_8 . For each sample the recorded dynamics were independent of detection wavelength.

(44) Elsaesser, T.; Kaiser, W. *Annu. Rev. Phys. Chem.* **1991**, *42*, 83–107.